

2006

Establishment of Polarity during Organization of the Acentrosomal Plant Cortical Microtubule Array

Ram Dixit

Pennsylvania State University - Main Campus, ramdixit@WUSTL.EDU

Eric Chang

Baylor College of Medicine

Richard Cyr

Pennsylvania State University - Main Campus

Follow this and additional works at: https://openscholarship.wustl.edu/bio_facpubs



Part of the [Biology Commons](#)

Recommended Citation

Dixit, Ram; Chang, Eric; and Cyr, Richard, "Establishment of Polarity during Organization of the Acentrosomal Plant Cortical Microtubule Array" (2006). *Biology Faculty Publications & Presentations*. 26.

https://openscholarship.wustl.edu/bio_facpubs/26

This Article is brought to you for free and open access by the Biology at Washington University Open Scholarship. It has been accepted for inclusion in Biology Faculty Publications & Presentations by an authorized administrator of Washington University Open Scholarship. For more information, please contact digital@wumail.wustl.edu.

Establishment of Polarity during Organization of the Acentrosomal Plant Cortical Microtubule Array[□] [▽]

Ram Dixit,* Eric Chang,[†] and Richard Cyr*

*Biology Department, Penn State University, University Park, PA 16802; and [†]Department of Molecular and Cell Biology, The Breast Center, Baylor College of Medicine, Houston, TX 77030

Submitted September 16, 2005; Revised December 14, 2005; Accepted December 20, 2005
Monitoring Editor: J. Richard McIntosh

The plant cortical microtubule array is a unique acentrosomal array that is essential for plant morphogenesis. To understand how this array is organized, we exploited the microtubule (+)-end tracking activity of two *Arabidopsis* EB1 proteins in combination with FRAP (fluorescence recovery after photobleaching) experiments of GFP-tubulin to examine the relationship between cortical microtubule array organization and polarity. Significantly, our observations show that the majority of cortical microtubules in ordered arrays, within a particular cell, face the same direction in both *Arabidopsis* plants and cultured tobacco cells. We determined that this polar microtubule coalignment is at least partially due to a selective stabilization of microtubules, and not due to a change in microtubule polymerization rates. Finally, we show that polar microtubule coalignment occurs in conjunction with parallel grouping of cortical microtubules and that cortical array polarity is progressively enhanced during array organization. These observations reveal a novel aspect of plant cortical microtubule array organization and suggest that selective stabilization of dynamic cortical microtubules plays a predominant role in the self-organization of cortical arrays.

INTRODUCTION

A fundamental aspect of microtubule (MT) array organization in all eukaryotes is the spatial organization of MT polarity. The best characterized mechanism driving MT organization requires a MT organizing center, such as a centrosome, which initiates MT polymerization and anchors these MTs with their (+)-ends radiating outward (Ou and Rattner, 2004; Varmark, 2004). However, this mechanism does not seem to operate to organize the plant cortical MT array because higher plants lack traditional centrosomes (Schmit, 2002). The acentrosomal plant cortical MT array is nonetheless capable of adopting several organizational states (Dixit and Cyr, 2004a; Lloyd and Chan, 2004), which play pivotal roles in plant morphogenesis and regulate both cell division and cell elongation events (Mineyuki, 1999; Wasteneys, 2004).

Plant cortical MTs are plasma membrane associated dynamic structures (Dixit and Cyr, 2004a) that are nucleated from dispersed sites throughout the cortex (Wasteneys and Williamson, 1989; Yuan *et al.*, 1994; Granger and Cyr, 2001; Shaw *et al.*, 2003). Significantly, the (–)-ends of these MTs are unanchored and consequently both MT ends are dynamic with the (+)-ends showing dynamic instability and the (–)-ends undergoing slow depolymerization, collec-

tively known as hybrid treadmilling (Shaw *et al.*, 2003). The polymer dynamics of plant cortical MTs can be described by stochastic parameters, which by themselves do not explain how cortical MT organization can occur. Recently, it was shown that the stochastic cortical MT dynamics are deterministically modified by the angle at which they encounter one another (Dixit and Cyr, 2004b). These deterministic events provide a mechanistic route that results in the parallel arrangement of cortical MTs; however, the relationship between MT polarity and organization in cortical MT arrays is not well understood.

To study the relationship between MT polarity and organization, we utilized the *Arabidopsis* End Binding 1 (EB1) family of MT-binding proteins because EB1 proteins are best known for their ability to bind MT (+)-ends (Bisgrove *et al.*, 2004; Akhmanova and Hoogenraad, 2005). The *Arabidopsis* EB1 protein family consists of three members, EB1a, EB1b, and EB1c (Chan *et al.*, 2003; Mathur *et al.*, 2003), which show between 82 and 47% overall amino acid sequence similarity to one another. The N-termini (1–133 amino acids) of EB1a and EB1b are ~93% similar and they are ~73% similar to the N-terminus of EB1c. In comparison, the C-termini of EB1a and EB1b are ~71% similar and they are ~32% similar to the C-terminus of EB1c. EB1a and EB1b are also more similar to human and yeast EB1 orthologues (30–35%), compared with EB1c (20–30%). Predictably, EB1a and b proteins would make ideal MT (+)-end markers; however, earlier studies using overexpressed proteins surprisingly showed that they extensively bind MTs and result in (–)-end (Chan *et al.*, 2003) and endomembrane (Mathur *et al.*, 2003) labeling.

In this study, we engineered both *Arabidopsis* and tobacco plant cells to stably express GFP (green fluorescent protein)-tagged EB1a and b at the proper levels of expression in order to better analyze cortical MT organization. We show that under low expression conditions, GFP-tagged EB1a and b, as expected, exclusively bind the (+)-end of MTs. With this tool, we demonstrated that the majority of MTs in organized

This article was published online ahead of print in *MBC in Press* (<http://www.molbiolcell.org/cgi/doi/10.1091/mbc.E05-09-0864>) on December 28, 2005.

□ ▽ The online version of this article contains supplemental material at *MBC Online* (<http://www.molbiolcell.org>).

Address correspondence to: Richard Cyr (rjc8@psu.edu).

Abbreviations used: MT, microtubule; EB1, end binding 1; GFP, green fluorescent protein; BY-2, bright yellow-2; FRAP, fluorescence recovery after photobleaching.

cortical arrays, in a given cell, have the same polarity and that the polar arrangement of cortical MTs occurs simultaneously with parallel MT arrangement. Finally, we present evidence that the polar MT alignment involves a selective stabilization of MTs of the same polarity and that MT polymerization rates do not substantially influence this process.

MATERIALS AND METHODS

Plant Transgenic Constructs and Transformation

The *EB1a*, *b*, and *c*-GFP fusion constructs were generated using recombinant PCR with the following primers: 5' *EB1a*, GGATCCATGGCGACGAA-CATCGGA; 3' *EB1a*, TCCGGTTGTTGCGGGCGCTTGAGCTCTTTTCTTC; 5' *EB1b*, GGATCCATGGCGACGAACATTGGGATG; 3' *EB1b*, TCCGGTTGTTGCGGCAGTTTGGGTCTCTGCAGC; 5' *EB1c*, GGATCCATGGCTACGAA-CATTGGGATG; 3' *EB1c*, TCCGGTTGTTGCGGGCAGGTCAAGAGAGGA-GA; 5' GFP, GCCGCAACAACCGGAGCATGAGTAAAGGAGAAGAAC; 3' GFP, GAGCTCTTATCCCGCTTGTATAG. All constructs were confirmed by sequencing and subsequently cloned downstream of a *HSP18.2* promoter (Takahashi *et al.*, 1992) in the pCambia1300 vector and introduced into *Nicotiana tabacum* L. cv. Bright Yellow-2 cells and *Arabidopsis thaliana* var. Columbia plants using *Agrobacterium*-mediated transformation. The *EB1b*-GFP construct was also cloned downstream of the *EB1b* promoter (1.5-kb sequence upstream of the *EB1b* start codon) in the pCambia1300 vector and was introduced into *A. thaliana* plants using *Agrobacterium*-mediated transformation. Transformed cells and plants were selected using 25 mg/l hygromycin, and independent transformants were used for subsequent analyses.

Heat-shock induction was achieved by exposing BY-2 cells (25 ml of cells in a 125-ml flask at 100 rpm rotation) and *Arabidopsis* plants (in a humid chamber) to 34°C for 2 h. Preliminary experiments showed that this treatment regime did not perturb cell growth, MT dynamics, or mitotic index. Although this treatment was mild, we routinely followed heat shock with recovery for at least 3 h at room temperature before conducting observations.

Yeast Rescue Experiments

A *mal3* null mutant (Chen *et al.*, 2000) was transformed with the thiamine-repressible pREP1 vector control or pREP1-containing *Arabidopsis EB1* orthologues or *mal3* as the positive control. Transformed cells were selected on appropriate minimal medium containing thiamine (20 μ M). Colonies of cells were pregrown in thiamine-free medium overnight to log phase before being serially diluted (1:5) and spotted on plates containing thiabendazole (TBZ) or the solvent (dimethyl sulfoxide) control. The standard yeast methods were as described (Chen *et al.*, 2000).

Microscopy

BY-2 cells, 2–3 d after subculture, were observed by immobilizing them on poly-L-lysine-coated coverslips in a humid chamber. Two- to 3-d-old *Arabidopsis* seedlings were observed by mounting them on poly-L-lysine-coated slides in distilled water. Images were collected using either a 40 \times (1.2 NA) C-Apochromat or 100 \times (1.3 NA) Plan-Neofluar, objective (Zeiss, Thornwood, NY).

Wide-field microscopy was conducted with a Zeiss Axiovert S100 TV microscope. Images were captured with a CoolSNAP HQ camera (Roper Scientific, Tucson, AZ) using 20–30% light intensity from a 100 W mercury arc-lamp and GFP (460–500-nm excitation, 510–560-nm emission) filter set at 5–10-s intervals using 1-s exposure times over a 5–10-min period. MT orientation was quantified by determining the angle of MT growth relative to the long axis of the cell. For these measurements, up to 20° difference in MT angles was considered to represent the same direction because MT encounters at this angle resulted in MT coalignment 90% of the time (Dixit and Cyr, 2004b). MTs that started out at divergent angles at the beginning of the movie but which subsequently became coaligned with other MTs after MT encounters were considered to be oriented in the same direction. However, if a rare MT changed direction more than 20° at the end of the movie, it was scored as a divergent MT.

Confocal microscopy was conducted with a Zeiss 510 Meta laser scanning microscope. The 488-nm laser line, at 3–5% power output, was selected for GFP excitation, and images were collected using 1-s scan times. For the fluorescence recovery after photobleaching (FRAP) experiments, photobleaching was achieved using three scans at 100% laser power, followed by image acquisition using 3% laser power at 3-s intervals.

RESULTS

Sequence Diversity and Specialization among the Arabidopsis EB1 Proteins

One evolutionarily conserved and important property of EB1 proteins is the ability to bind the (+)-ends of MTs

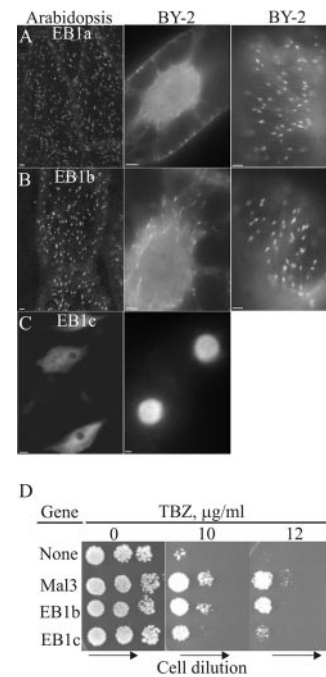


Figure 1. Characterization of *Arabidopsis EB1* proteins. Localization of EB1a-GFP (A), EB1b-GFP (B), and EB1c-GFP (C) in *Arabidopsis* plants and cultured BY-2 cells. *EB1* gene expression was driven using the inducible *HSP18.2* promoter. The first and third columns of the figure show an optical slice through the cortex, and the second column shows a midplane optical slice. In D, fission yeast *mal3* null mutant expressing indicated genes were pregrown to log phase and then serially diluted (1:5) and spotted on plates containing either the solvent control or an anti-MT drug, TBZ. Colony formation was documented after 4 d of incubation at 30°C. Scale bars, 2 μ m.

(Bisgrove *et al.*, 2004; Akhmanova and Hoogenraad, 2005) with high affinity; additionally, a lower affinity interaction has also been observed along the sidewalls of MTs (Tirnauer *et al.*, 2002). An earlier report by Chan *et al.* (2003), who used a strong 35S promoter, did reveal the sidewall binding to plant MTs and hence we asked if the use of weaker and/or endogenous promoters would allow more exclusive reporting of the MT (+)-ends. To investigate whether the *Arabidopsis EB1* proteins can associate with MT (+)-ends, under low expression conditions, we generated transgenic *Arabidopsis* plants expressing either EB1a, b, or c fused with GFP under the control of the *HSP18.2* inducible promoter, which allows for fine-tuning of EB1 expression. Under this carefully controlled condition, we found that EB1a-GFP and EB1b-GFP exclusively show cometlike structures (i.e., the signal has an asymmetric axial distribution, with the brightest signal emanating from the leading edge; $0.98 \pm 0.15 \mu$ m for EB1a and $0.99 \pm 0.13 \mu$ m for EB1b) that appear to move rapidly in the cell (Figures 1, A and B, and Supplementary Movie 1). These EB1-comets disappear upon treatment with a MT depolymerizing agent, propyzamide, but not with latrunculin-B, which induces F-actin depolymerization (Supplementary Figure 1). In contrast to EB1a and b, induced EB1c-GFP does not show cometlike MT labeling and instead it is localized to the nucleus (Figure 1C).

To determine whether the EB1-GFP localization patterns are conserved across plant families, EB1-GFP proteins were similarly expressed in stably transformed tobacco BY-2 cells. Our data showed that, as in *Arabidopsis*, low expressing

EB1a-GFP and EB1b-GFP appeared in a cometlike pattern ($1.01 \pm 0.11 \mu\text{m}$ for EB1a; $1.11 \pm 0.18 \mu\text{m}$ for EB1b; $n = 50$; Figure 1, A and B, and Supplementary Movie 2), whereas EB1c-GFP is nuclear (Figure 1C). The cometlike character, with the bright side leading has been shown to be diagnostic of (+)-end growth (Tirnauer *et al.*, 2002) and in all instances this behavior was observed in plant cells that expressed EB1 at low levels. In addition, during mitosis, EB1a-GFP and EB1b-GFP comets are seen to migrate toward and accumulate at the spindle midzone (i.e., away from the spindle poles), which is consistent with MT (+)-end localization because (+)-ends extensively interdigitate in this area of the spindle. Accumulation was not observed at the spindle poles (Supplementary Movie 3). EB1a-GFP and EB1b-GFP are indistinguishable in terms of comet growth velocity ($5.10 \pm 0.7 \mu\text{m}/\text{min}$ vs. $4.98 \pm 0.78 \mu\text{m}/\text{min}$; $n = 100$ MTs, respectively). Notably, in contrast to the low expression conditions, high expression of EB1b-GFP in BY-2 cells, using the 35S promoter, results in loss of (+)-end-labeling specificity and more extensive labeling of MTs, which indicates the lower affinity sidewall binding site is present in plant EB1 (Supplementary Figure 2).

To further investigate whether functions of EB1 are evolutionarily conserved, we examined whether EB1 can rescue MT defects in fission yeast that lack the EB1 ortholog Mal3. As shown in Figure 1D, *mal3* null cells are hypersensitive to drugs that destabilize MTs, such as TBZ (Chen *et al.*, 2000), and this defect is more efficiently rescued by EB1b and only weakly rescued by EB1c.

Collectively, we concluded from these results that EB1a and EB1b, like the mammalian and yeast counterparts, display a strong MT (+)-end binding activity under low expression conditions, whereas EB1c is a more divergent form.

EB1 Reveals Polar MT Arrangement within Organized Cortical MT Arrays

The MT (+)-end localization of EB1a-GFP and EB1b-GFP provided a tool to examine the MT (+)-end distribution in the crowded plant cortical MT array.

In isodiametric BY-2 cells, the EB1a-GFP and EB1b-GFP comets are oriented in random directions, suggesting that these MTs are not organized and thus displaying random MT (+)-end polarity (Supplementary Figure 3 and Supplementary Movie 4). However, in elongated BY-2 cells, the EB1a-GFP and EB1b-GFP markers revealed that the majority of MT (+)-ends ($76 \pm 12\%$ with EB1a; >600 microtubules; and $79 \pm 13\%$ with EB1b; >800 microtubules; 10 cells each) are oriented transversely with the same polarity (Figure 2A and Supplementary Movie 5). Moreover, optical sectioning of these cells showed that the cortical MT (+)-end polarity is continuous along all faces of the cell (i.e., the polarity is observed circumferentially about the cell; unpublished data).

To better understand this phenomenon in organized tissues, we also analyzed *Arabidopsis* plants that were stably transformed with a construct expressing EB1b-GFP, under the control of the native *EB1b* promoter, and found that epidermal cells containing transverse (indicative of a rapid elongative state) or longitudinal (indicative of tissues that have ceased elongating; Dixit and Cyr, 2004a) cortical arrays also display polar ($76 \pm 9\%$; >500 microtubules; 12 cells; 5 independent lines) MT (+)-end organization (Figure 2B and Supplementary Movie 6).

Using the same analytical approach as with the cultured BY-2 cells, we closely examined cells in these organized tissues (i.e., all cells had ordered cortical MTs) and observed an interesting pattern in which $\sim 70\%$ of cells with organized

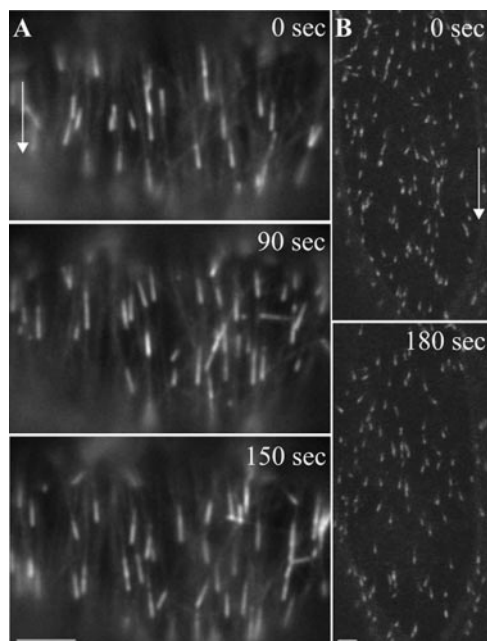


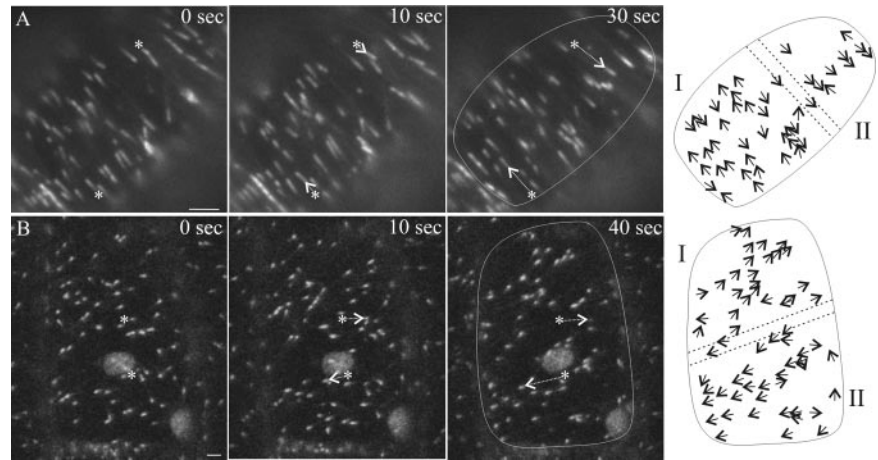
Figure 2. Net global array polarity within ordered cortical MT arrays under conditions of low expression. Cultured BY-2 cells stably expressing *HSP18.2* promoter-driven EB1b-GFP (A) and T_3 generation *Arabidopsis* plants stably expressing *EB1b* promoter-driven EB1b-GFP (B) were observed using wide-field ($100\times$ objective) to show the axial asymmetry of comet fluorescence) and confocal laser scanning fluorescence microscopy ($40\times$ objective to show a wider field of comets), respectively. A subset of snapshots from a time-lapse series is shown. The majority of comets, 90% in A and $\sim 85\%$ in B, are oriented in the same direction in these two cells (indicated by arrows). Scale bar, $2 \mu\text{m}$.

cortical MT arrays exhibit global cortical array polarity; that is, the same net MT polarity was observed in all regions of the cortex in these cells. Furthermore, the net cortical MT array polarity appeared to be cell autonomous, i.e., one cell can contain MTs of one polarity, while its neighbor can contain MTs of the opposite polarity. In the remaining 30% of cells with organized cortical MT arrays, regional variation in net MT polarity was observed. In such cells, distinguishable belts or hoops of opposing MT polarity occur in the cell cortex (Figure 3, A and B). In these cells, we noted a boundary area where MT dynamics appeared somewhat depressed as judged by a lower frequency of comets in this area. These boundary regions were not included in our quantitative analyses. Similar to cells with global MT array polarity, the net polarity within individual belts of MT polarity is $\sim 80\%$ on average. In all cases, we typically observed the same net organization in neighboring cells (i.e., similar net transverse, oblique, or longitudinal arrangement) but the net direction of microtubule polarity could differ.

FRAP Analysis of β -Tubulin Also Shows MT Polarity in Ordered Cortical Arrays

To determine whether the cortical MT organization, as detected by EB1 labeling, properly represents all the MTs in the cortex, we sought to examine the organization of MT polarity in *Arabidopsis* plants by tracking the direction of β -tubulin 6 (TUB6) polymerization, which takes place at the (+)-end of the MT. To this end, we performed FRAP to first photobleach a segment of cortical MTs labeled by GFP-TUB6

Figure 3. Regional sectors of polarity within ordered cortical MT arrays. EB1b-GFP in BY-2 cells and *Arabidopsis* plants were analyzed microscopically as described in Figure 2. The asterisks mark specific MT comets to illustrate how growth trajectory was assessed (shown by the dotted arrows). The polarity of the cortical MTs in the last image is represented diagrammatically in the last panel. MT polarity bias is concentrated in different parts of the same cell (designated as sectors I and II). The dotted lines show the boundary areas not included in the quantization. Sector I in A shows 70% polarity oriented facing the top-left; whereas sector II shows 82% polarity oriented in the opposite direction. Similarly, sector I in B shows 79% polarity oriented facing the top-right, whereas sector II shows 77% polarity oriented in the opposite direction. Scale bar, 2 μ m.



(Nakamura *et al.*, 2004) and then examined the polarity of these MTs by tracking the direction in which fluorescence recovery occurred. In agreement with previous studies (Hush *et al.*, 1994; Yuan *et al.*, 1994; Shaw *et al.*, 2003), we found that the photobleached MTs recovered fully within 2–3 min, confirming the high turnover of cortical MTs. In support of our EB1 studies, we observed that in the photobleached region, the majority of the MTs ($70 \pm 10\%$; >500 MTs; 25 cells) are of the same polarity. This is true of cells with longitudinal (Figure 4A and Supplementary Movie 7) and transverse (Figure 4B and Supplementary Movie 8) arrays. Therefore, polar coalignment of cortical MTs is a general property of parallel MT organization.

Selective Coalignment of MTs Is Associated with Selective MT Stability

We next examined how selective MT (+)-end alignment might be established. We asked if MTs with the same polarity are somehow selectively more stable than those MTs with opposite polarity. This quantification was performed by tracking individual EB1 comets appearing from within 1 μ m of the cell edge and determining their duration before they disappeared (due to MT pause or catastrophe) or exited the field of view at the other edge. Comet loss due to MT pause or catastrophe was distinguishable from the occasional MT comets coming in and out of the focal plane because comet loss occurred asymmetrically starting from the tail of the comet to the distal end, whereas, MTs coming in and out of the focal plane were distinguishable by the progressive blurring or sharpening of the entire comet. Only those comets that remained within the focal plane during their lifespan were included in the quantification. These data are a measure of the duration of MT growth because EB1 dissociates from the ends of paused or depolymerizing MTs.

Our data obtained from EB1b-GFP-expressing BY-2 cells (Supplementary Figure 4) show that the average “lifespan” of the comets is significantly greater among MTs oriented in the majority direction (85 ± 15 s vs. 67 ± 11 s; p -value of 0.002 using t test; >500 MTs). MT comets oriented in the majority direction frequently followed the tracks of previous comets (Supplementary Figure 4), consistent with MT bundling following shallow-angle MT encounters (Dixit and Cyr, 2004b). On the other hand, MT comets oriented in the minority direction frequently disappeared after encountering MT comets growing in the majority direction. These observations are consistent with the hypothesis that cortical MT array polarity is established through selective stabiliza-

tion (and therefore enrichment) of copolar MTs compared with antiparallel MTs. We found no significant difference in the comet velocities between MTs of opposing directions, suggesting that MT polymerization rate is not the mechanism leading to net cortical array polarity.

Progressive Establishment of Array Polarity during Cortical MT Array Organization

To understand the sequence of events leading to the establishment of cortical array polarity, newly forming cortical MT arrays were examined in 10 recently divided EB1b-GFP-expressing BY-2 cells. After the completion of cytokinesis, EB1b-GFP comets populate the cortex in multiple orientations as newly nucleated cortical MTs appear (Figure 5; panel 10 min). In the initial stages of cortical array formation (~ 30 min after cytokinesis), MTs headed in multiple directions and typically only 30–40% MT (+)-end coalignment was observed (panel 30 min). In the subsequent stages of array organization, the number of discordantly oriented MTs decreases, whereas the number of transversely aligned MTs increases with no significant change in the total number of MTs (panels 45 min to 240 min). Simultaneously, the number of MTs with coaligned (+)-ends increases, ultimately resulting in a net ($\sim 80\%$), but not absolute, cortical MT array polarity. This trend was consistently observed in all 10 cells and the Kolmogorov-Smirnov test confirmed that the distribution of MT angles after the completion of cytokinesis is significantly ($p \sim 0.005$) different from the distribution of MT angles 3 h after the completion of cytokinesis. These results suggest that to order cortical MTs, the population of MTs with the same polarity gradually enriches as more randomly oriented MTs become parallel to one another.

DISCUSSION

Although the organization of MTs by the centrosome elegantly explains how many MT structures are assembled, it is challenging to envision how organized MT arrays may be assembled without a centrosome. The plant cortical MT arrays thus represent an ideal model system to study such an event. Our data show that MTs in these arrays, in a given cell, are organized such that they predominantly project with the same polarity. Our data further illustrated that the ordering of cortical MTs occurs soon after cortical MT nucleation at the end of cytokinesis, during which MTs with the same polarity gradually enrich and become parallel to

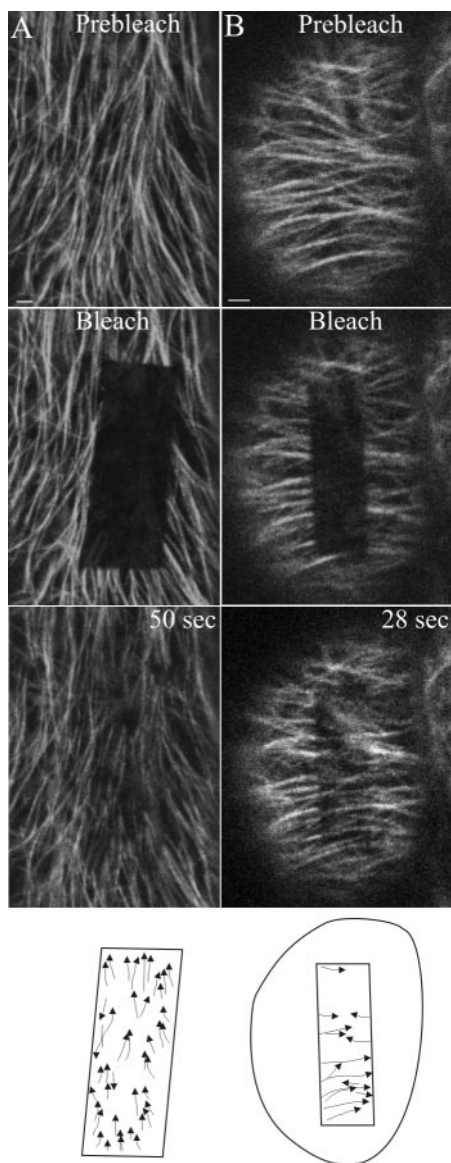


Figure 4. FRAP analysis of MT (+)-end orientation in ordered arrays. *Arabidopsis* plants expressing GFP-TUB6 were used to determine the orientation of cortical MT (+)-ends in longitudinal (A) and transverse (B) arrays using confocal laser scanning microscopy. GFP fluorescence was bleached using three scans at 100% 488-nm laser power and fluorescence recovery monitored by collecting images at 3-s intervals using 3% laser power. The polarity of the cortical MTs in the last image is represented diagrammatically in the last panel. The fluorescence recovery pattern shows 90% directionality bias in A and 80% directionality bias in B. This is best viewed in the Supplementary Movies. Scale bar, 2 μ m.

one another. Finally, we revealed that cortical MT array polarity is associated with selective stabilization of MTs oriented in the majority direction.

The study of densely packed cortical MTs has been hindered by the lack of good MT end markers. Our study suggests that EB1a or EB1b is a powerful tool for this type of analysis, provided that they are properly expressed. At low expression levels, we observed that EB1a and EB1b primarily label growing MT (+)-ends throughout the cell cycle, whereas at high levels they extensively decorate MT side-

walls. This difference in how EB1 interacts with MTs, dependent on the level of expression, is consistent with the idea that EB1 has two binding sites for MTs: one with high-affinity that is specific for (+)-end labeling and one with lower affinity specific for binding to the sidewall. Data in support of this comes from work with budding yeast and *Xenopus* (Tirnauer and Bierer, 2000; Schuyler and Pellman, 2001; Tirnauer *et al.*, 2002) and here we show a similar phenomenon, which indicates the duality in MT interactions is likely an evolutionary conserved feature of EB1 proteins. We did not detect any (–)-end labeling by EB1a and EB1b as was reported by Chan *et al.* (2003), who worked with cells that were expressing high levels of EB1. This difference in how plant EB1 interacts with MTs most likely is due to the difference in protein expression levels because native promoter-driven, low-level EB1 expression by the same group also did not result in MT (–)-end labeling (Chan *et al.*, 2005).

Our studies with plant EB1 also reveal that EB1c may in fact represent a new member of the EB1 family, with a distinct function, because it does not associate with the (+)-ends of cortical MTs but rather shows nuclear localization during interphase and spindle and phragmoplast localization during mitosis (Van Damme *et al.*, 2004a and our unpublished results). Furthermore, it does not replace yeast EB1 as efficiently as EB1b. Because EB1c diverges most extensively from other EB1 proteins in the C-terminus, we speculate that the C-terminus of EB1 proteins can impart specific functions shared by a given EB1 subfamily.

The observed polarity of cortical MTs was first deduced from studying EB1 and later it was corroborated by FRAP experiments on GFP-TUB6. Both techniques effectively sample the entire cortical MT array based on the well-established fact that plant cortical MTs are highly dynamic. Although the EB1 markers localize only to growing (+)-ends, they are expected to label all cortical MTs at some point during our observation period because of the high dynamicity and rescue frequency of cortical MTs (Chan *et al.*, 2003; Dhonukshe and Gadella, 2003; Mathur *et al.*, 2003; Shaw *et al.*, 2003; Dixit and Cyr, 2004b; Nakamura *et al.*, 2004; Van Damme *et al.*, 2004a; Vos *et al.*, 2004; Abe and Hashimoto, 2005). We specifically confirmed the high dynamicity of cortical MTs by performing FRAP analyses on GFP-TUB6 that showed complete recovery of photobleached MTs within 2–3 min. Therefore, we are confident that the described organization of MTs is a general feature of the cortical array and is not influenced by which marker was used for the analysis.

Although we have demonstrated that organized cortical MTs, in a given cell, have a predominant polarity, some previous reports suggested that cortical MT arrays do not have a well-defined polarity after examining MTs data sets pooled from many cells (Shaw *et al.*, 2003; Tian *et al.*, 2004; Vos *et al.*, 2004). Our study provides some important clues to allow for a better understanding of these conflicting conclusions. First, tracking MT dynamics using GFP-tubulin, rather than using an end marker, can underestimate the extent of MT coalignment because of limitations in sampling MTs in a crowded environment. It is difficult to resolve growing (+)-ends of bundled MTs using GFP-tubulin, whereas, the (+)-ends of bundled MTs are easily detectable by EB1-GFP as discrete comets. Furthermore, MTs oriented in the same direction frequently track along existing MTs (Dhonukshe *et al.*, 2005) and therefore, predictably, remain unresolved when observed using GFP-tubulin. In addition, our study found that MT coalignment is readily detectable in elongated cells, whereas cells that are nearly spherical do not exhibit such coalignment. Finally, in ~30% of cells with

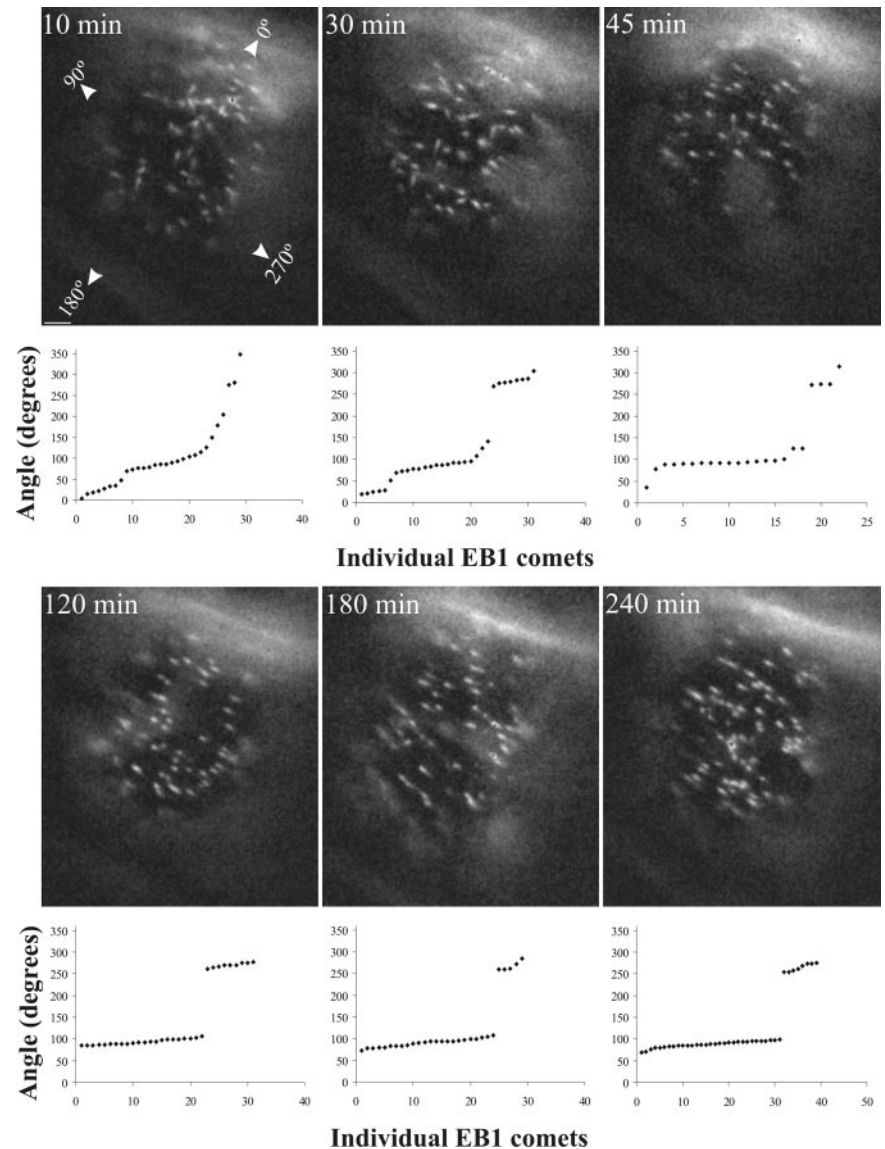


Figure 5. Cortical microtubule ordering and polarity in a recently divided BY-2 cell. A cultured BY-2 cell stably expressing *HSP18.2* promoter-driven EB1b-GFP was observed after completion of cytokinesis to follow the pattern of cortical MT array organization and polarity. Images acquired at different times are accompanied by scatter plots of the direction in which the individual EB1b-GFP comets are headed. The angles of the comet trajectories were measured relative to the long axis of the cell (in degrees). The progressive acquisition of MT parallelism is closely associated with the establishment of net array polarity ($\sim 90^\circ$ in this cell). The Kolmogorov-Smirnov test showed that the distribution of MT angles is statistically indistinguishable from 10 min up to 45 min ($p \sim 0.5$), but becomes statistically significant from 120 min onward ($p \sim 0.001$) in this cell. Scale bar, 2 μm .

array polarity, their MTs can be divided into two or more regions of opposing polarity. Hence, in about one third of cells there is no “net” coalignment of MTs along the entire cell. Although hook decoration of cortical MTs suggested mixed MT polarity (Tian *et al.*, 2004), it is important to highlight that the authors also noted that only 30% of cortical MTs were hook decorated (Tian *et al.*, 2004). Because of this technical limitation, this study relied on quantification of MT polarity by pooling data obtained from small sample sets (3–6 MTs) from numerous different cells. Because we have reported here that the net MT polarity can vary from cell to cell, pooling data from large numbers of cells will predictably give the impression of mixed polarity. In support of our observations, examination of the literature shows undiscussed cases of net MT polarity within plant cortical MT arrays. For example, Figure 2D in Chan *et al.* (2003) shows $\sim 74\%$ net MT polarity; and, Figure 1B in Dhonukshe *et al.* (2005) shows $\sim 75\%$ net MT polarity. Furthermore, analyses of serial electron micrograph sections from individual cells also show that adjacent cortical MT ends share a common directionality (Hardham and Gunning, 1978).

In terms of the mechanism of polar coalignment of cortical MTs, our data show that cortical MT array polarity is established progressively after MT nucleation at the end of cytokinesis and is concomitant with the parallel ordering of cortical MTs. Cortical MT nucleation predominantly occurs from existing cortical MTs in a γ -tubulin-dependent manner (Murata *et al.*, 2005). This MT-dependent nucleation results in branching patterns of cortical MTs (Falconer *et al.*, 1988; Wasteneys and Williamson, 1989; Wasteneys, 2002; Murata *et al.*, 2005) that are subsequently resolved into coaligned cortical MTs, probably due to intermicrotubule interactions (Dixit and Cyr, 2004b). Specifically, branching MTs colliding with neighboring MTs at shallow angles would become bundled and stabilized, whereas, those MTs colliding with neighboring MTs are steep angles would depolymerize and be lost from the population. Over time, these intermicrotubule interactions foster the generation of coaligned cortical MTs (Dixit and Cyr, 2004b). In this scheme, selective stabilization of cortical MTs in a particular direction would mean that subsequent MTs nucleated from these “pioneer” MTs would possess roughly the same polarity and eventually

resolve into a polar coaligned array. In support of this hypothesis, we show that as MTs achieve coalignment, there is an enrichment of MTs with the same polarity relative to those with the opposite polarity, and our data show that this process is associated with a selective stabilization of copolar MTs, and not by any change in MT polymerization rate. From a molecular standpoint, MT crossing-linking proteins, such as MAP65 isoforms, may facilitate the process of aligning MTs that are close to one another. Indeed, AtMAP65-1 and AtMAP65-5 predominantly decorate coaligned cortical MTs (Van Damme *et al.*, 2004b; Mao *et al.*, 2005) and it will be interesting to determine whether these MTs have uniform polarity.

From the perspective of the cortical MT array function, we speculate that the cortical MT array polarity influences the polar deposition of cellulose wall microfibrils, which themselves are polar polymers (i.e., the reducing ends of the β -1,4 glucan chains are oriented distal to the cellulose synthase complex). The inherent polarity of these two interacting systems (i.e., MTs and cellulose) may play an integral role in the cross-talk between these two systems (Fisher and Cyr, 1998). One possibility is that cellulose synthase complexes interact, in some manner, with the cortical MT array in a chiral manner, as suggested by the unidirectional microfibril deposition by groups of cellulose synthase complexes (Brown and Montezinos, 1976; Herth, 1984; Kudlicka *et al.*, 1987; Delmer and Amor, 1995; Tsekos *et al.*, 1999). The predilection for unidirectional higher order cellulose microfibril bundles also suggests polar microfibril deposition (Brett, 2000). In addition, the *Arabidopsis* *FRA1* (Fragile fiber 1) gene encodes a kinesinlike protein with predicted (+)-end motor activity that is required for the oriented deposition of cellulose microfibrils (Zhong *et al.*, 2002), consistent with the idea that polarity within the cortical MT array is conveyed to the cellulose microfibril array. This notion suggests we rethink the paradigm of simple coalignment between MTs and microfibrils and extend it to encompass their mutual, polar coalignment.

ACKNOWLEDGMENTS

We thank Imelda Mercado for her expert help with the yeast rescue experiments and Takashi Hashimoto for GFP-TUB6-expressing *Arabidopsis* plants. Work in the Chang lab is supported by a National Institutes of Health grant (CA90464) and work in the Cyr lab is supported by a DOE grant (DE-FG02-91ER20050).

REFERENCES

- Abe, T., and Hashimoto, T. (2005). Altered microtubule dynamics by expression of modified alpha-tubulin protein causes right-handed helical growth in transgenic *Arabidopsis* plants. *Plant J.* 43, 191–204.
- Akhmanova, A., and Hoogenraad, C. C. (2005). Microtubule plus-end-tracking proteins: mechanisms and functions. *Curr. Opin. Cell Biol.* 17, 47–54.
- Bisgrove, S. R., Hable, W. E., and Kropf, D. L. (2004). +TIPs and microtubule regulation. The beginning of the plus end in plants. *Plant Physiol.* 136, 3855–3863.
- Brett, C. T. (2000). Cellulose microfibrils in plants: biosynthesis, deposition, and integration into the cell wall. *Int. Rev. Cytol.* 199, 161–199.
- Brown, R. M., Jr., and Montezinos, D. (1976). Cellulose microfibrils: visualization of biosynthetic and orienting complexes in association with the plasma membrane. *Proc. Natl. Acad. Sci. USA* 73, 143–147.
- Chan, J., Calder, G. M., Doonan, J. H., and Lloyd, C. W. (2003). EB1 reveals mobile microtubule nucleation sites in *Arabidopsis*. *Nat. Cell Biol.* 5, 967–971.
- Chan, J., Calder, G. M., Fox, S., and Lloyd, C. W. (2005). Localization of the microtubule end binding protein EB1 reveals alternative pathways of spindle development in *Arabidopsis* suspension cells. *Plant Cell* 17, 1737–1748.

- Chen, C. R., Chen, J., and Chang, E. C. (2000). A conserved interaction between Moe1 and Mal3 is important for proper spindle formation in *Schizosaccharomyces pombe*. *Mol. Biol. Cell* 11, 4067–4077.
- Delmer, D. P., and Amor, Y. (1995). Cellulose biosynthesis. *Plant Cell* 7, 987–1000.
- Dhonukshe, P., and Gadella, T. W., Jr. (2003). Alteration of microtubule dynamic instability during preprophase band formation revealed by yellow fluorescent protein-CLIP170 microtubule plus-end labeling. *Plant Cell* 15, 597–611.
- Dhonukshe, P., Mathur, J., Hulskamp, M., and Gadella, T. W., Jr. (2005). Microtubule plus-ends reveal essential links between intracellular polarization and localized modulation of endocytosis during division-plane establishment in plant cells. *BMC Biol.* 3, 11.
- Dixit, R., and Cyr, R. (2004a). The cortical microtubule array: from dynamics to organization. *Plant Cell* 16, 2546–2552.
- Dixit, R., and Cyr, R. (2004b). Encounters between dynamic cortical microtubules promote ordering of the cortical array through angle-dependent modifications of microtubule behavior. *Plant Cell* 16, 3274–3284.
- Falconer, M., Donaldson, G., and Seagull, R. (1988). MTOCs in higher plant cells: an immunofluorescent study of microtubule assembly sites following depolymerization by APM. *Protoplasma* 144, 46–55.
- Fisher, D. D., and Cyr, R. J. (1998). Extending the microtubule/microfibril paradigm—cellulose synthesis is required for normal cortical microtubule alignment in elongating cells. *Plant Physiol.* 116, 1043–1051.
- Granger, C. L., and Cyr, R. J. (2001). Spatiotemporal relationships between growth and microtubule orientation as revealed in living root cells of *Arabidopsis thaliana* transformed with green-fluorescent-protein gene construct GFP-MBD. *Protoplasma* 216, 201–214.
- Hardham, A. R., and Gunning, B.E.S. (1978). Structure of cortical microtubule arrays in plant cells. *J. Cell Biol.* 77, 14–34.
- Herth, W. (1984). Oriented “rosette” alignment during cellulose formation in mung bean hypocotyl. *Naturwissenschaften* 71, 216.
- Hush, J. M., Wadsworth, P., Callaham, D. A., and Hepler, P. K. (1994). Quantification of microtubule dynamics in living plant cells using fluorescence redistribution after photobleaching. *J. Cell Sci.* 107, 775–784.
- Kudlicka, K., Wardrop, A., Itoh, T., and Brown, R. (1987). Further evidence from sectioned material in support of the existence of a linear terminal complex in cellulose synthesis. *Protoplasma* 136, 96–103.
- Lloyd, C., and Chan, J. (2004). Microtubules and the shape of plants to come. *Nat. Rev. Mol. Cell Biol.* 5, 13–22.
- Mao, T., Jin, L., Li, H., Liu, B., and Yuan, M. (2005). Two microtubule-associated proteins of the *Arabidopsis* MAP65 family function differently on microtubules. *Plant Physiol.* 138, 654–662.
- Mathur, J., Mathur, N., Kernebeck, B., Srinivas, B. P., and Hulskamp, M. (2003). A novel localization pattern for an EB1-like protein links microtubule dynamics to endomembrane organization. *Curr. Biol.* 13, 1991–1997.
- Mineyuki, Y. (1999). The preprophase band of microtubules: its function as a cytokinetic apparatus in higher plants. *Int. Rev. Cytol.* 187, 1–49.
- Murata, T., Sonobe, S., Baskin, T. I., Hyodo, S., Hasezawa, S., Nagata, T., Horio, T., and Hasebe, M. (2005). Microtubule-dependent microtubule nucleation based on recruitment of gamma-tubulin in higher plants. *Nat. Cell Biol.* 7, 961–968.
- Nakamura, M., Naoi, K., Shoji, T., and Hashimoto, T. (2004). Low concentrations of propyzamide and oryzalin alter microtubule dynamics in *Arabidopsis* epidermal cells. *Plant Cell Physiol.* 45, 1330–1334.
- Ou, Y., and Rattner, J. B. (2004). The centrosome in higher organisms: structure, composition, and duplication. *Int. Rev. Cytol.* 238, 119–182.
- Schmit, A. C. (2002). Acentrosomal microtubule nucleation in higher plants. *Int. Rev. Cytol.* 220, 257–289.
- Schuyler, S. C., and Pellman, D. (2001). Microtubule “plus-end-tracking proteins”: the end is just the beginning. *Cell* 18, 421–424.
- Shaw, S. L., Kamyar, R., and Ehrhardt, D. W. (2003). Sustained microtubule treadmill in *Arabidopsis* cortical arrays. *Science* 300, 1715–1718.
- Takahashi, T., Naito, S., and Komeda, Y. (1992). The *Arabidopsis* *HSP18.2* promoter/GUS gene fusion in transgenic *Arabidopsis* plants: a powerful tool for the isolation of regulatory mutants of the heat-shock response. *Plant J.* 2, 751–761.
- Tian, G. W., Smith, D., Gluck, S., and Baskin, T. I. (2004). Higher plant cortical microtubule array analyzed in vitro in the presence of the cell wall. *Cell Motil. Cytoskeleton.* 57, 26–36.

- Tirnauer, J. S., and Bierer, B. E. (2000). EB1 proteins regulate microtubule dynamics, cell polarity, and chromosome stability. *J. Cell Biol.* *15*, 761–766.
- Tirnauer, J. S., Grego, S., Salmon, E. D., and Mitchison, T. J. (2002). EB1-microtubule interactions in *Xenopus* egg extracts: role of EB1 in microtubule stabilization and mechanisms of targeting to microtubules. *Mol. Biol. Cell* *13*, 3614–3626.
- Tsekos, I., Orogas, N., and Herth, W. (1999). Cellulose microfibril assembly and orientation in some bangiophyte red algae: relationship between synthesizing terminal complexes and microfibril structure, shape, and dimensions. *Phycologia* *38*, 217–224.
- Van Damme, D., Bouget, F. Y., Van Poucke, K., Inze, D., and Geelen, D. (2004a). Molecular dissection of plant cytokinesis and phragmoplast structure: a survey of GFP-tagged proteins. *Plant J.* *40*, 386–398.
- Van Damme, D., Van Poucke, K., Boutant, E., Ritzenthaler, C., Inze, D., and Geelen, D. (2004b). In vivo dynamics and differential microtubule-binding activities of MAP65 proteins. *Plant Physiol.* *136*, 3956–3967.
- Varmark, H. (2004). Functional role of centrosomes in spindle assembly and organization. *J. Cell. Biochem.* *91*, 904–914.
- Vos, J. W., Dogterom, M., and Emons, A. M. (2004). Microtubules become more dynamic but not shorter during preprophase band formation: a possible “search-and-capture” mechanism for microtubule translocation. *Cell Motil. Cytoskelet.* *57*, 246–258.
- Wasteneys, G. O. (2002). Microtubule organization in the green kingdom: chaos or self-order? *J. Cell Sci.* *115*, 1345–1354.
- Wasteneys, G. O. (2004). Progress in understanding the role of microtubules in plant cells. *Curr. Opin. Plant Biol.* *7*, 651–660.
- Wasteneys, G. O., and Williamson, R. E. (1989). Reassembly of microtubules in *Nitella tasmanica*: quantitative analysis of assembly and orientation. *Eur. J. Cell Biol.* *50*, 76–83.
- Yuan, M., Shaw, P. J., Warn, R. M., and Lloyd, C. W. (1994). Dynamic reorientation of cortical microtubules, from transverse to longitudinal, in living plant cells. *Proc. Natl. Acad. Sci. USA* *91*, 6050–6053.
- Zhong, R., Burk, D. H., Morrison, W. H., 3rd, and Ye, Z. H. (2002). A kinesin-like protein is essential for oriented deposition of cellulose microfibrils and cell wall strength. *Plant Cell* *14*, 3101–3117.